Divertor-core integration in high-performance, negative triangularity plasmas on TCV

G. Durr-Legoupil-Nicoud, O. Février, C. Contré, R. Morgan, O. Sauter, C. Theiler, K. Lee, S. Coda, A. Perek, H. Reimerdes, E. Tonello, B. Vincent, M. Zurita, the TCV[a] and the EUROfusion Tokamak Exploitation teams[b]

Ecole Polytechnique Fédérale de Lausanne (EPFL), Swiss Plasma Center (SPC), CH-1015 Lausanne, Switzerland.

b. See the author list of B.P. Duval et al. 2024 Nucl. Fusion 64 112023.

c. See the author list of E. Joffrin et al. 2024 Nucl. Fusion 64 112019.

Introduction

Negative Triangularity (NT) promises reactor-relevant scenarios with high core confinement while operating in L-mode, thus robustly avoiding H-mode and edge-localized modes (ELMs) [1,2]. However, experiments on TCV [4] and DIII-D [3,5] have shown that detachment is less accessible in NT than in Positive Triangularity (PT), due to factors such as the divertor geometry, lower neutral pressure in the divertor, and a narrower scrape-off layer resulting from non-X-point shaping [4,5,6,8]. To overcome these limitations, Alternative Divertor Configurations (ADCs) such as the Snowflake (SF) divertor have been developed in recent years. These aim to ease access to detachment by splitting strike points and increasing both the connection length and magnetic flux expansion [7]. In this work, we focus on exploiting the SF divertor to achieve detachment in NT configurations, first in ohmic density ramp experiments, and then in high-performance scenarios using nitrogen (N_2) seeding.

Snowflake divertor and ohmic detachment

The discharges used for the comparison have an LSN and SF divertor, Figure 1a. Both have a closed divertor and ohmic heating and a non-X-point triangularity of $\delta_{NXP} \sim -0.3$. For this study, the ion ∇B drifts are directed downward, i.e. are favorable for accessing H-mode. Density ramps are performed from $\langle n_e \rangle \sim 4 \times 10^{19}$m^{-3} to disruption. The SF configuration disrupts at $\langle n_e \rangle \sim 9.8 \times 10^{19}$m^{-3} while the LSN at $\langle n_e \rangle \sim 8.2 \times 10^{19}$m^{-3}. Plasma-baffle interaction is minimal, with less than 5% of the ion flux reaching the surface of the baffles. The SF configuration has a 1.5 mm separation between the two separatrices, remapped upstream, smaller than the power fall-off length of 3 ± 1 mm typical of TCV ohmic discharges with $\delta_{NXP} \sim -0.3$ [8].

The SF configuration leads to a 50% increase in neutral pressure within the divertor in comparison to the LSN divertor, Figure.1b. It also results in a lower effective charge (Z_{eff}), indicating reduced core plasma impurity contamination, Fig.1c. The core electron density and temperature profiles are similar for both the SF and the LSN configuration. Bolometric measurements reveal the formation of an X-point radiator, with the radiation around the X-point moving into the core plasma region.

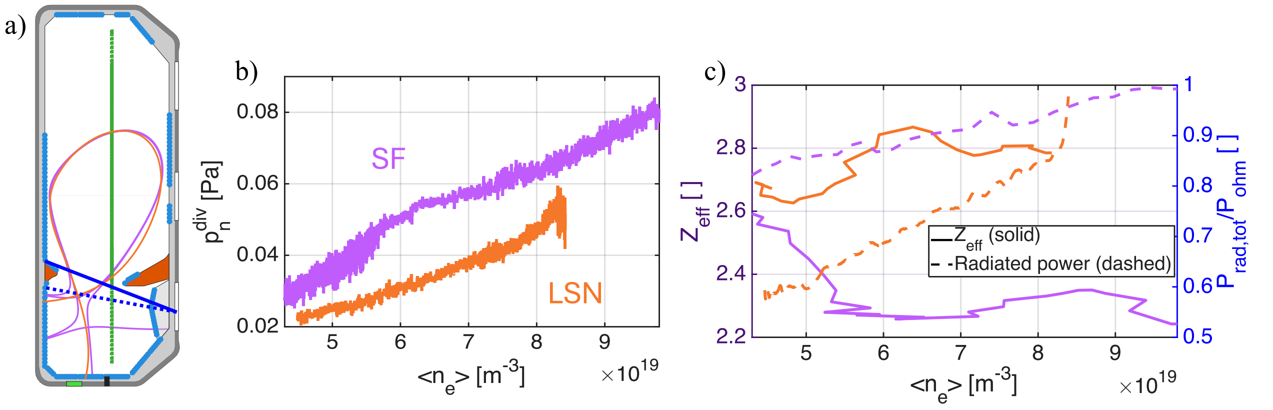

Figure 1: (a) Poloidal cross section of TCV with LSN and SF separatrices (resp. orange and purple). The light blue dots are the Langmuir probes' positions, the blue solid and dashed lines mark the range of bolometry lines of sight used, the green squares are the Thomson scattering measurement locations, and the black is the APG (Asdex Pressure Gauge) location. (b) Divertor neutral pressure measured by the APGs, (c) effective charge number (solid lines, left axis) and radiated fraction of the input ohmic power (dashed lines, right axis) for LSN (orange) and SF (purple) configurations as a function of the line-averaged electron density.

All SF strike points reached electron temperatures below 10 eV, Figure 2a. A roll-over in ion flux was observed at SP1 and SP2, while SP4 showed saturation of the ion flux, Figure 2b. The strike points of the SF configuration are numbered from 1 to 4, counterclockwise from the high to the low-field side of the tokamak. SP3 exhibits negligible flux. In contrast, the LSN configuration exhibits

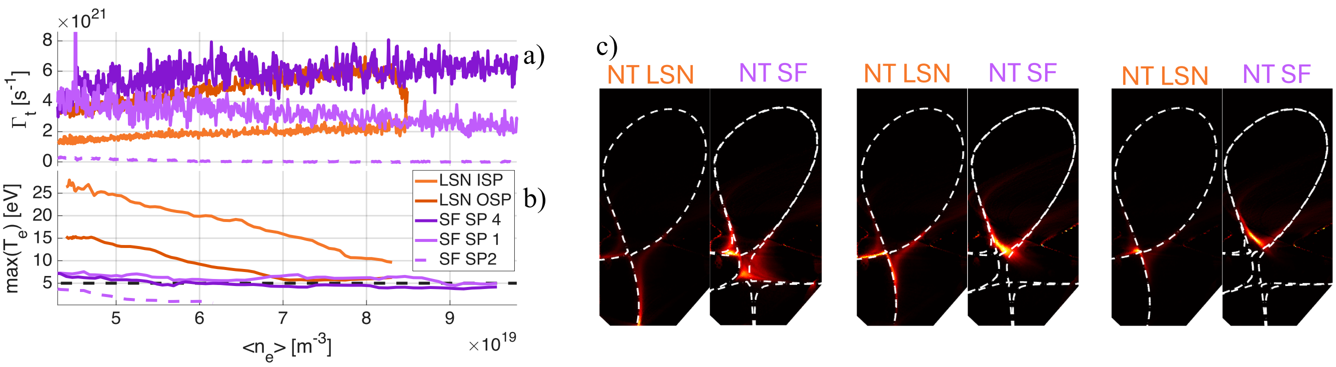

Figure 2: (a) Integral ion flux and (b) maximum electron temperature at the target as a function of the line-averaged electron density measured by the Langmuir probes. (c) Tomographic inversions of the MANTIS measurements of the CIII emission at 3 line-averaged electron densities.

electron temperatures below 10 eV only at the outer strike point (OSP), and the ion flux at this target decreases only shortly before the disruption. The overall heat flux is significantly lower in the SF configuration (not shown). The CIII emission front, measured by the MANTIS diagnostic, is observed to move toward the X-point in both the LSN and SF cases (not shown). However, only in the SF configuration does the divertor cool entirely below 10 eV. Full detachment of the ohmic NT SF configuration is observed across all diagnostics from $\langle n_e \rangle \sim 9 \times 10^{19}$m^{-3} where the LSN configuration only approaches detachment at the OSP before disrupting.

Development of high-power NT snowflake scenario

As the SF divertor allows reaching detachment of all strike points in ohmic density ramps, it is leveraged to obtain a high-performance detached NT scenario. During scenario development, vertical instability was a challenge, , as well as strong fueling through Neutral Beam Heating (NBH), which sometimes led uncontrolled rises in plasma density, likely triggered by increased particle confinement. High-performance NT discharge using NBH1 with 550 kW of injected power and a plasma current of 170 kA were nevertheless achieved, Figure 3. H-mode-like confinement was reached with H_{98} reaching values up to 1.5. The average core density is $\langle n_e \rangle \sim 4.5 \times 10^{19}$m^{-3}, corresponding to a Greenwald fraction of f_G=0.4. A nitrogen seeding ramp starts at t = 1.6 s to achieve detachment. For the power exhaust study, minimal plasma-wall interaction in ensured with a 3 cm gap maintained between the LCFS (last closed field surface) and the vessel walls. As in the ohmic cases, plasma-baffle interactions are limited to less than 5% of the total flux reaching the targets.

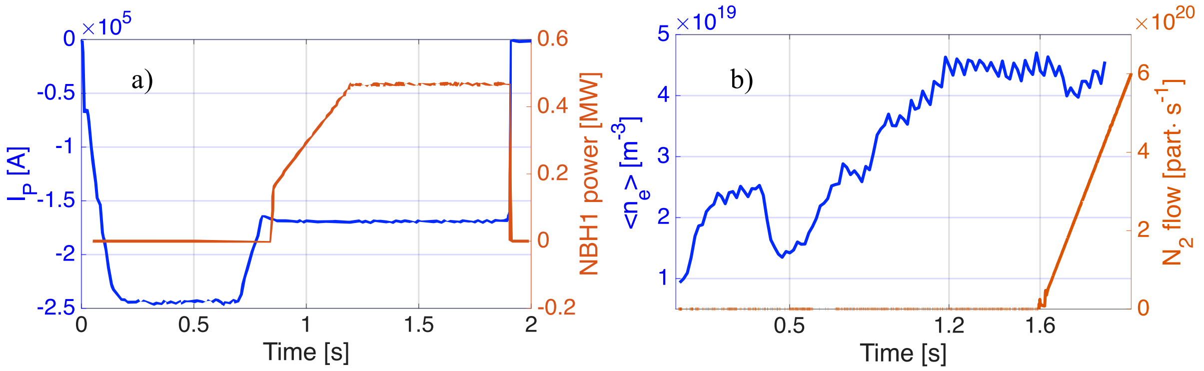

Figure 3: (a) Time traces of the plasma current, NBH heating power, as well as (b) line-averaged electron density and N_2 flow for the high-power baffled NT SF discharge (#83575)

Power exhaust and core performance in high-power scenario

As shown in Fig. 4a, most of the particle flux is directed to SP1 and SP4. During N_2 seeding, ion fluxes decrease at all the strike points. The seeding leads to divertor cooling below 5 eV at SP2, SP3, and SP4. At SP1, the temperature peaks at 8 eV shortly before the disruption. A clear formation of an X-point radiator is observed with bolometry at high seeding (not shown). Before disruption, the CIII front position is close to the X-point, as seen by the MANTIS diagnostic, indicating that the entire divertor region cools below 10 eV. Detachment was achieved at SP2, SP3, and SP4, while SP1 approached detachment at $< n_e >\sim 4.5 \times 10^{19}$ m^{-3} and 8.8×10^{22} of injected N_2 particles. The plasma exhibits H-mode-like confinement. The core temperature is 10% higher than in TCV's PT H-mode cases, while the normalized beta is about 20% lower. Seeding has a measurable impact on the core plasma, with a slight reduction in energy confinement and an increase in core dilution (Z_{eff} rising from 2.0 to 2.4).

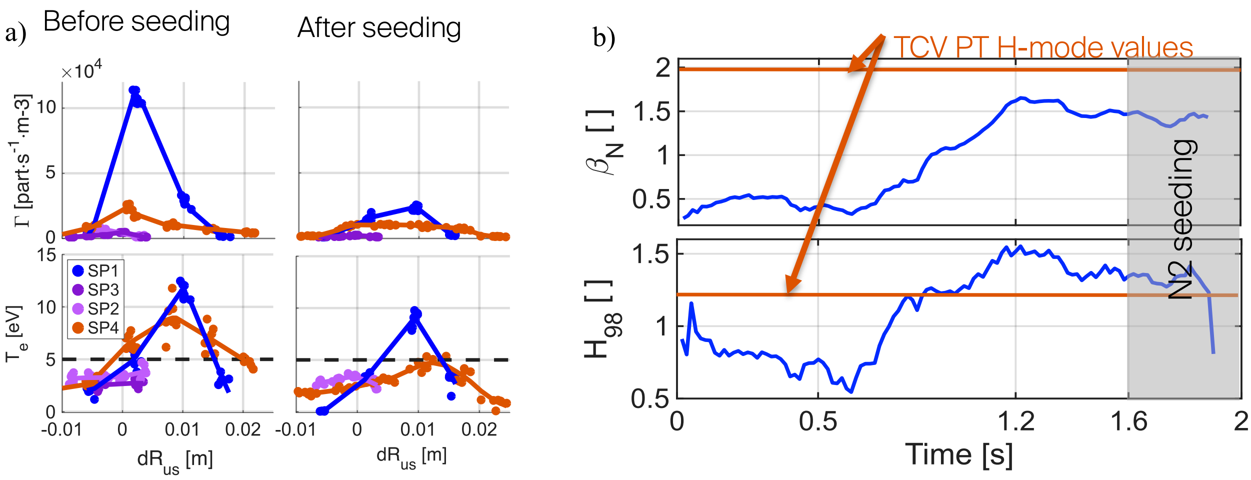

Figure 4: (a) Ion flux and electron temperature profiles at SP1, 2, 3 and 4 before and after N_2 seeding of the high-power NT SF discharge. (b) Normalized beta and H_{98} values during the discharge (blue) and TCV PT H-mode typical values (orange)

Conclusion & outlook

Operation with a baffled SF divertor enables detachment at all divertor targets during NT ohmic density ramps, while only the OSP reaches sub-5 eV temperatures in NT LSN discharges. A newly developed high-power NT scenario with a SF divertor achieves core performance levels comparable to those seen in PT LSN H-mode plasmas. Nitrogen seeding enables the cooling of SP1 and detachment of all other strike points, with a minor impact on core performance. The next step will focus on mitigating the performance degradation observed during detachment in NT plasmas, aiming to optimize detached scenarios without compromising core confinement.

References

[1] S. Coda et al, *Plasma Phys. Control. Fusion*, **64** 014004 (2022)

[2] A. O. Nelson et al, *PRL,* **131** 195101 (2023)

[3] K. E. Thome et al, *Plasma Phys. Control. Fusion* **66** 105018 (2024)

[4] O. Février et al, *Plasma Phys. Control. Fusion*, **66** 065005 (2024)

[5] F. Scotti *et al*, *Nucl. Fusion* **64** 094001 (2024)

[6] G. Durr-Legoupil-Nicoud et al, in prep. (2025)

[7] S. Gorno et al , *Plasma Phys. Control. Fusion*, **65** 035004 (2023)

[8] R. Morgan, submitted to *Nuclear Fusion* (2025)